MTRT - A Modified Transverse Resonance Technique

Alfrêdo Gomes Neto †, Creso S. da Rocha ‡, Hervé Aubert #, D. Bajon #, H. Baudrand #
†CEFET-PB, Av. 1 de maio, 720, João Pessoa, PB, 58015-430, BRAZIL
‡DEE, UFPB, Cx.Postal 10053, Campina Grande, PB, 58109-970, BRAZIL
Lab. d'Electronique, ENSEEIHT, 2 rue C. Chamichel, Toulouse, FRANCE

Abstract — **In this work a modified formulation of the transverse resonance technique (TRT) is presented. The difference between the usual TRT and the formulation presented here, MTRT, is the equivalent network considered. With the MTRT proposed formulation, mode solution identification requires less arduous work. The complete equation set is described. Numerical results are presented for dispersion characteristics of microstrip lines, coupled microstrip lines and conductor-backed coplanar waveguides (CBCW). When compared to results obtained by other methods, a good agreement is observed.**

I. INTRODUCTION

The recent developments made in microwave and millimeter-wave circuits (MIC), especially in the monolithic form (MMIC) where it is very difficult to tune the circuits once they are fabricated, have required extremely accurate computer aided design (CAD) programs [1]. Along with this, the considerable advances in computers have allowed a rapid evolution of the usual numerical techniques. In this sense, a modified formulation of the transverse resonance technique (MTRT) is presented in this work. One of the advantages of the MTRT, when compared to the usual TRT, is the possibility of analyzing open side structures exactly, without the use of auxiliary geometry, which permits considerable reduction in the work for mode solutions identification. Numerical results are presented for dispersion characteristics of microstrip lines, coupled microstrip lines and conductor-backed coplanar waveguides (CBCW). When compared to results obtained by other methods, a good agreement is observed.

II. THEORY

In the conventional formulation of the TRT, a suitable equivalent network is established, representing discontinuity planes and boundary conditions, to compute the cutoff frequencies and possibly some additional characteristics of the structures [2]. The difference between the conventional and the modified TRT is the equivalent network adopted. In the TRT, the discontinuity planes are parallel to the conductor strips (Fig. 1), whereas in the MTRT they are perpendicular (Fig. 2). Figures 1 and 2 present equivalent networks and respective matrix admittances for a microstrip. Mode coupling, that occurs at each discontinuity, is represented by generic voltage sources. The different transmission line sections represent the different waveguide sections (in the MTRT case, two homogeneous waveguides (a and b) and one inhomogeneous (cd)). The admit-

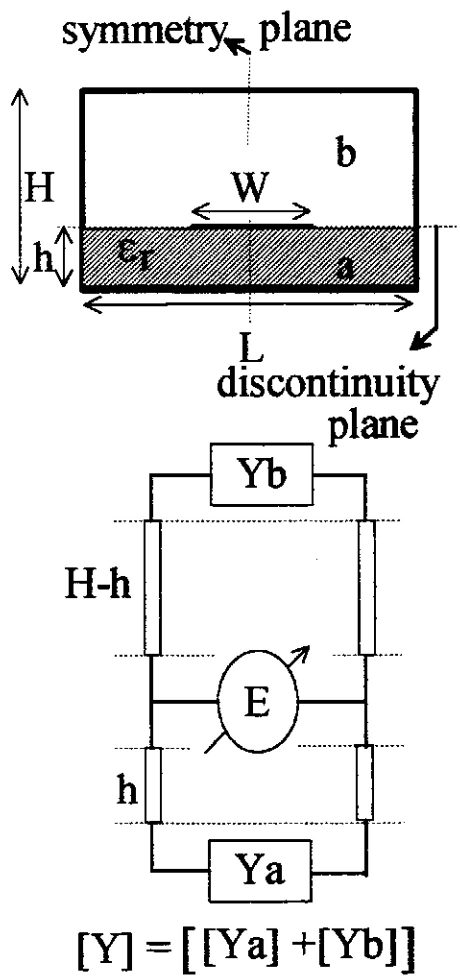

Figure 1: TRT

tances ($Y_{a,b,cd}$) represent the boundary conditions.

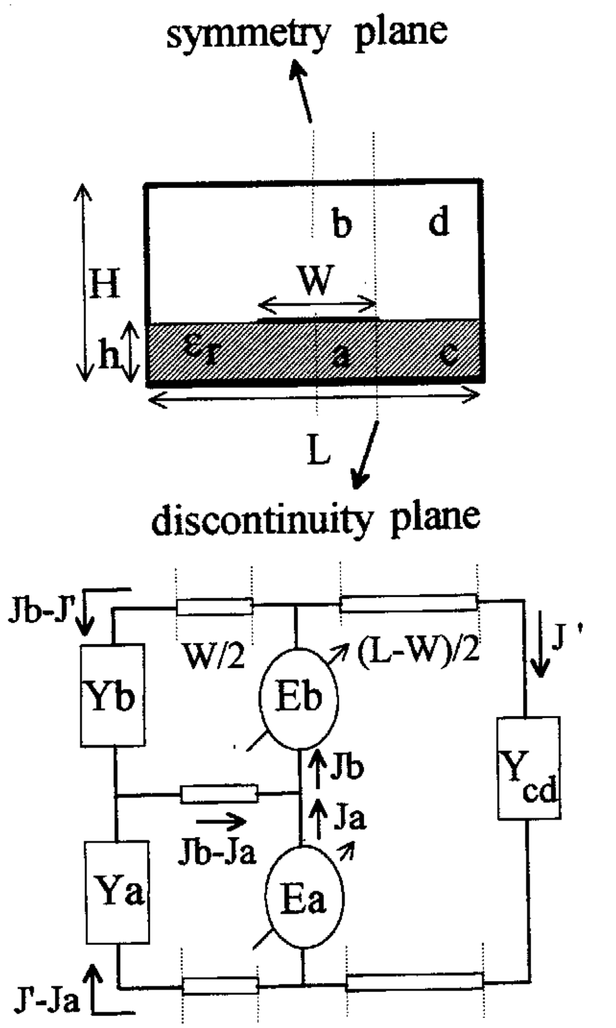

$$[Y] = \begin{bmatrix} [Ya]+[Y^{a}_{cd}] & [Y^{ab}_{cd}] \\ [Y^{ba}_{cd}] & [Yb]+[Y^{b}_{cd}] \end{bmatrix}$$

Figure 2: MTRT

The matrix admittance $[Y]$ is obtained by the use of Kirchhoff's laws and it is deduced in the following way:

$$[J_a] - [J'] = [Y_a][E_a] \qquad (1)$$

$$[J_b] - [J'] = [Y_b][E_b] \qquad (2)$$

$$[J'] = [Y_{cd}]([E_a] + [E_b]) \qquad (3)$$

Substituing (3) into (1) and (2) yields

$$[J_a] - ([Y_{cd}]([E_a] + [E_b])) = [Y_a][E_a] \qquad (4)$$

$$[J_b] - ([Y_{cd}]([E_a] + [E_b])) = [Y_b][E_b] \qquad (5)$$

The equations (4) and (5) can be rewritten as

$$[J_a] = ([Y_a] + [Y_{cd}])[E_a] + [Y_{cd}][E_b] \qquad (6)$$

$$[J_b] = [Y_{cd}][E_a] + ([Y_b] + [Y_{cd}])[E_b] \qquad (7)$$

or in the matrix form

$$\begin{bmatrix} [J_a] \\ [J_b] \end{bmatrix} = \begin{bmatrix} ([Y_a] + [Y_{cd}]) & [Y_{cd}] \\ [Y_{cd}] & ([Y_b] + [Y_{cd}]) \end{bmatrix} \begin{bmatrix} [E_a] \\ [E_b] \end{bmatrix} \qquad (8)$$

If it is assumed that suitable inner products ($\langle\,|\,\rangle$) can be determined, equation (8) may be written as

$$\begin{bmatrix} [J_a] \\ [J_b] \end{bmatrix} = \begin{bmatrix} \langle\,|\,\rangle([Y_a] + [Y_{cd}])\langle\,|\,\rangle & \langle\,|\,\rangle[Y_{cd}]\langle\,|\,\rangle \\ \langle\,|\,\rangle[Y_{cd}]\langle\,|\,\rangle & \langle\,|\,\rangle([Y_b] + [Y_{cd}])\langle\,|\,\rangle \end{bmatrix} \begin{bmatrix} [e_a] \\ [e_b] \end{bmatrix} \qquad (9)$$

Note that when $\langle\,|\,\rangle[Y]_{cd}\langle\,|\,\rangle$ involves only testing function in the region $a(b)$ the notation $\langle\,|\,\rangle[Y^{a(b)}_{cd}]\langle\,|\,\rangle$ is adopted. The notation $\langle\,|\,\rangle[Y^{ab}_{cd}]\langle\,|\,\rangle$, or $\langle\,|\,\rangle[Y^{ba}_{cd}]\langle\,|\,\rangle$, is adopted to indicate that testing functions in regions a and b are used in the inner products. In Fig. 2, the inner product symbol, $\langle\,|\,\rangle$, is omitted. Matrix terms are detailed in the following equations.

$$[Y_{\nu_1}] = \sum_{n=0}^{n\nu_1} \begin{bmatrix} [Y_{\nu_1,n(yy)}] & [Y_{\nu_1,n(yz)}] \\ [Y_{\nu_1,n(zy)}] & [Y_{\nu_1,n(zz)}] \end{bmatrix} \qquad (10)$$

$$[Y_{\nu_1,n(yy)}] = \langle\phi_y^{\nu_1}|f_{y,n}^{\nu_1}\rangle Y_{\nu_1,n}\langle f_{y,n}^{\nu_1}|\phi_y^{\nu_1}\rangle \qquad (11)$$

$$\left[Y_{\nu_1,n(yz)}\right] = \langle \phi_y^{\nu_1} | f_{y,n}^{\nu_1} \rangle Y_{\nu_1,n} \langle f_{z,n}^{\nu_1} | \phi_z^{\nu_1} \rangle \qquad (12)$$

$$\left[Y_{\nu_1,n(zy)}\right] = \langle \phi_z^{\nu_1} | f_{z,n}^{\nu_1} \rangle Y_{\nu_1,n} \langle f_{y,n}^{\nu_1} | \phi_y^{\nu_1} \rangle \qquad (13)$$

$$\left[Y_{\nu_1,n(zz)}\right] = \langle \phi_z^{\nu_1} | f_{z,n}^{\nu_1} \rangle Y_{\nu_1,n} \langle f_{z,n}^{\nu_1} | \phi_z^{\nu_1} \rangle \qquad (14)$$

with $\nu_1 = a, b$

$$[Y_{cd}^a] = \sum_{n=0}^{na} \begin{bmatrix} \left[Y_{cd,n(yy)}^a\right] & \left[Y_{cd,n(yz)}^a\right] \\ \left[Y_{cd,n(zy)}^a\right] & \left[Y_{cd,n(zz)}^a\right] \end{bmatrix} \qquad (15)$$

$$\left[Y_{cd,n(yy)}^a\right] = \langle \phi_y^a | f_{y,n}^c \rangle Y_{cd,n} \langle f_{y,n}^c | \phi_y^a \rangle \qquad (16)$$

$$\left[Y_{cd,n(yz)}^a\right] = \langle \phi_y^a | f_{y,n}^c \rangle Y_{cd,n} \langle f_{z,n}^c | \phi_z^a \rangle \qquad (17)$$

$$\left[Y_{cd,n(zy)}^a\right] = \langle \phi_z^a | f_{z,n}^c \rangle Y_{cd,n} \langle f_{y,n}^c | \phi_y^a \rangle \qquad (18)$$

$$\left[Y_{cd,n(zz)}^a\right] = \langle \phi_z^a | f_{z,n}^c \rangle Y_{cd,n} \langle f_{z,n}^c | \phi_z^a \rangle \qquad (19)$$

$$[Y_{cd}^b] = \sum_{n=0}^{nb} \begin{bmatrix} \left[Y_{cd,n(yy)}^b\right] & \left[Y_{cd,n(yz)}^b\right] \\ \left[Y_{cd,n(zy)}^b\right] & \left[Y_{cd,n(zz)}^b\right] \end{bmatrix} \qquad (20)$$

$$\left[Y_{cd,n(yy)}^b\right] = \langle \phi_y^b | f_{y,n}^d \rangle Y_{cd,n} \langle f_{y,n}^d | \phi_y^b \rangle \qquad (21)$$

$$\left[Y_{cd,n(yz)}^b\right] = \langle \phi_y^b | f_{y,n}^d \rangle Y_{cd,n} \langle f_{z,n}^d | \phi_z^b \rangle \qquad (22)$$

$$\left[Y_{cd,n(zy)}^b\right] = \langle \phi_z^b | f_{z,n}^d \rangle Y_{cd,n} \langle f_{y,n}^d | \phi_y^b \rangle \qquad (23)$$

$$\left[Y_{cd,n(zz)}^b\right] = \langle \phi_z^b | f_{z,n}^d \rangle Y_{cd,n} \langle f_{z,n}^d | \phi_z^b \rangle \qquad (24)$$

$$[Y_{cd}^{ab}] = \sum_{n=0}^{na} \begin{bmatrix} \left[Y_{cd,n(yy)}^{ab}\right] & \left[Y_{cd,n(yz)}^{ab}\right] \\ \left[Y_{cd,n(zy)}^{ab}\right] & \left[Y_{cd,n(zz)}^{ab}\right] \end{bmatrix} \qquad (25)$$

$$\left[Y_{cd,n(yy)}^{ab}\right] = \langle \phi_y^a | f_{y,n}^c \rangle Y_{cd,n} \langle f_{y,n}^d | \phi_y^b \rangle \qquad (26)$$

$$\left[Y_{cd,n(yz)}^{ab}\right] = \langle \phi_y^a | f_{y,n}^c \rangle Y_{cd,n} \langle f_{z,n}^d | \phi_z^b \rangle \qquad (27)$$

$$\left[Y_{cd,n(zy)}^{ab}\right] = \langle \phi_z^a | f_{z,n}^c \rangle Y_{cd,n} \langle f_{y,n}^d | \phi_y^b \rangle \qquad (28)$$

$$\left[Y_{cd,n(zz)}^{ab}\right] = \langle \phi_z^a | f_{z,n}^c \rangle Y_{cd,n} \langle f_{z,n}^d | \phi_z^b \rangle \qquad (29)$$

$$[Y_{cd}^{ba}] = \sum_{n=0}^{nb} \begin{bmatrix} \left[Y_{cd,n(yy)}^{ba}\right] & \left[Y_{cd,n(yz)}^{ba}\right] \\ \left[Y_{cd,n(zy)}^{ba}\right] & \left[Y_{cd,n(zz)}^{ba}\right] \end{bmatrix} \qquad (30)$$

$$\left[Y_{cd,n(yy)}^{ba}\right] = \langle \phi_y^b | f_{y,n}^d \rangle Y_{cd,n} \langle f_{y,n}^c | \phi_y^a \rangle \qquad (31)$$

$$\left[Y_{cd,n(yz)}^{ba}\right] = \langle \phi_y^b | f_{y,n}^d \rangle Y_{cd,n} \langle f_{z,n}^c | \phi_z^a \rangle \qquad (32)$$

$$\left[Y_{cd,n(zy)}^{ba}\right] = \langle \phi_z^b | f_{z,n}^d \rangle Y_{cd,n} \langle f_{y,n}^c | \phi_y^a \rangle \qquad (33)$$

$$\left[Y_{cd,n(zz)}^{ba}\right] = \langle \phi_z^b | f_{z,n}^d \rangle Y_{cd,n} \langle f_{z,n}^c | \phi_z^a \rangle \qquad (34)$$

where:

$\phi_{\nu_2}^{\nu_1}$ are testing functions that satisfy boundary conditions in the discontinuity planes, in region $\nu_1(\nu_1 = a, b)$, on the axis $\nu_2(\nu_2 = y, z)$.

$f_{\nu_2,n}^{\nu_3}$ is the n^{th} basis function, which describe the electric and magnetic fields in the region ν_3, on the axis $\nu_2(\nu_2 = y, z)$.

Y_{ν_4} is the admittance, that represents the boundary conditions of the transmission line section, shifted to the discontinuity plane, in the region $\nu_4(\nu_4 = a, b, cd)$.

The adopted testing functions are:

$$\phi^{a,b}_{y,n} = \sqrt{\zeta_n/h'}\cos(n\pi y'/h') \qquad (35)$$

$$\phi^{a,b}_{z,n} = \sqrt{\zeta_n/h'}\sin(n\pi y'/h') \qquad (36)$$

$$h' = \begin{cases} h, & a \\ & for \\ (H-h), & b \end{cases} \qquad (37)$$

$$\gamma_y = n.\pi/h' \qquad (38)$$

$$y' = \begin{cases} y, & a \\ & for \\ (H-y) & b \end{cases} \qquad (39)$$

$$\zeta_n = \begin{cases} 1, & n \ even \\ & for \\ 2, & n \ odd \end{cases} \qquad (40)$$

As the regions a and b correspond to homogeneous waveguides, the basis functions are TE and TM electric field equations, on the axis y and z.

TE modes,

$$f^{a,b}_{y,n} = e^{a,b}_{y,n} = \left(\frac{-\gamma_z\sqrt{\zeta_n/h'}}{\sqrt{\kappa_1(\kappa_2+\gamma_y^2)}}\right)\cos(\gamma_y y')e^{-\gamma_z z} \qquad (41)$$

$$f^{a,b}_{z,n} = e^{a,b}_{z,n} = \left(\frac{\gamma_y\sqrt{\zeta_n/h'}}{\sqrt{\kappa_1(\kappa_2+\gamma_y^2)}}\right)\sin(\gamma_y y')e^{-\gamma_z z} \qquad (42)$$

TM modes,

$$f^{a,b}_{y,n} = e^{a,b}_{y,n} = \left(\jmath\frac{\gamma_y}{\gamma_z}\frac{\sqrt{\zeta_n/h'}}{\sqrt{\kappa_1(\kappa_2+\gamma_y^2)}}\right)\cos(\gamma_y y')e^{-\gamma_z z} \qquad (43)$$

$$f^{a,b}_{z,n} = e^{a,b}_{z,n} = \left(-\jmath\frac{\sqrt{\zeta_n/h'}\sqrt{\kappa_2}}{\sqrt{\kappa_1(\kappa_2+\gamma_y^2)}}\right)\sin(\gamma_y y')e^{-\gamma_z z} \qquad (44)$$

For the regions c and d that correspond to inhomogeneous waveguides, the basis functions are LSE and LSM electric current density ($\vec{J} = -\sqrt{\frac{\mu_0}{\epsilon_0}}\vec{H}\times\vec{a_x}$) field equations [2], on the axis y and z.

LSE modes,

$$f^{c}_{y,n} = J^{c}_{y,n} = \left(\frac{\cosh(\xi_{y,2}h'')}{\cosh(\xi_{y,1}h)}\right)\left(\frac{\xi_{y,2}}{\jmath K_0}\right)\left(\frac{\gamma_z}{\gamma_x}\right)\cosh(\xi_{y,1}y)e^{\gamma_{xz}} \qquad (45)$$

$$f^{c}_{z,n} = J^{c}_{z,n} = \left(\frac{\sinh(\xi_{y,2}h'')}{\sinh(\xi_{y,1}h)}\right)\left(\frac{\xi_{y,2}^2+K_0^2}{\jmath K_0\gamma_x}\right)\sinh(\xi_{y,1}y)e^{\gamma_{xz}} \qquad (46)$$

$$f^{d}_{y,n} = J^{d}_{y,n} = \left(\frac{\xi_{y,2}}{\jmath K_0}\right)\left(\frac{\gamma_z}{\gamma_x}\right)\cosh(\xi_{y,2}(H-y))e^{\gamma_{xz}} \qquad (47)$$

$$f^{d}_{z,n} = J^{d}_{z,n} = \left(\frac{\xi_{y,2}^2+K_0^2}{\jmath K_0\gamma_x}\right)\sinh(\xi_{y,2}(H-y))e^{\gamma_{xz}} \qquad (48)$$

LSM modes,

$$f^{c}_{y,n} = J^{c}_{y,n} = -\sqrt{\mu_0/\epsilon_0}\left(\frac{\cosh(\xi_{y,2}h'')}{\cosh(\xi_{y,1}h)}\right)\cosh(\xi_{y,1}y)e^{\gamma_{xz}} \qquad (49)$$

$$f^{c}_{z,n} = J^{c}_{z,n} = 0 \qquad (50)$$

$$f^{d}_{y,n} = J^{d}_{y,n} = -\sqrt{\mu_0/\epsilon_0}\cosh(\xi_{y,2}(H-y))e^{\gamma_{xz}} \qquad (51)$$

$$f^{d}_{z,n} = J^{d}_{z,n} = 0 \qquad (52)$$

with,

$$h'' = (H-h) \qquad (53)$$

$$e^{\gamma_{xz}} = e^{-(\gamma_x x+\gamma_z z)} \qquad (54)$$

$$\kappa_1 = e^{-\gamma_z z}.(e^{-\gamma_z z})^* \qquad (55)$$

$$\kappa_2 = \gamma_z.(\gamma_z)^* \qquad (56)$$

$$K_0 = \omega\sqrt{\mu_0\epsilon_r} \qquad (57)$$

$$\gamma^2_{x,a(b)} = -K_0^2\epsilon_{r,a(b)} - \gamma_z^2 + \gamma_y^2 \qquad (58)$$

and $\xi_{y,1}$ and $\xi_{y,2}$ are obtained from the solution of the following equation system:

$$\begin{cases} \xi_{y,1}\coth(\xi_{y,1}h) + \xi_{y,2}\coth(\xi_{y,2}h'') = 0 \\ \xi_{y,1}^2 \;+\; \xi_{y,2}^2 \;=\; K_0^2(1-\epsilon_r) \end{cases} \quad (59)$$

$$\begin{cases} \gamma_{x,cd}^2 \;=\; -(K_0^2\epsilon_r + \gamma_z^2 + \xi_{y,1}^2) \\ \quad\;\; = \; -(K_0^2 + \gamma_z^2 + \xi_{y,2}^2) \end{cases} \quad (60)$$

The admittances are defined as functions of the boundary conditions and are given by:

Electric symmetry

$$Y_{a(b),n}(x = W/2) = Y_n^{a(b)} \coth(\gamma_{x,a(b)}W/2) \quad (61)$$

Magnetic symmetry

$$Y_{a(b),n}(x = W/2) = Y_n^{a(b)} \tanh(\gamma_{x,a(b)}W/2) \quad (62)$$

with

$$Y_n^{a(b)} = \frac{\gamma_{x,a(b)}}{jK_0\epsilon_{r,a(b)}}, \quad TE \quad modes \quad (63)$$

$$Y_n^{a(b)} = \frac{jK_0\epsilon_{r,a(b)}}{\gamma_{x,a(b)}}, \quad TM \quad modes \quad (64)$$

For electric side walls

$$Y_n^{cd} = \frac{1}{N^*}\coth\left(\gamma_{x,cd}(L-W)/2\right) \quad (65)$$

with magnetic side walls

$$Y_n^{cd} = \frac{1}{N^*}\tanh\left(\gamma_{x,cd}(L-W)/2\right) \quad (66)$$

and for open sides structures

$$Y_n^{cd} = \frac{1}{N^*} \quad (67)$$

where $1/N^* = 1/\langle \vec{e}|\vec{j}\rangle$ is defined in [3], and given by:

LSE modes

$$N = \nu_1\left(\frac{\sinh(2\xi_{y,1}h)}{4\xi_{y,1}} - \frac{h}{2}\right)\left(\frac{\xi_{y,1}^*}{\xi_{y,1}}\right) + \nu_2\left(\frac{\sinh(2\xi_{y,2}h'')}{4\xi_{y,2}} - \frac{h''}{2}\right)\left(\frac{\xi_{y,2}^*}{\xi_{y,2}}\right) \quad (68)$$

LSM modes

$$N = \nu_3\left(\frac{\sinh(2\xi_{y,1}h)}{4\xi_{y,1}} + \frac{h}{2}\right) + \nu_4\left(\frac{\sinh(2\xi_{y,2}h'')}{4\xi_{y,2}} + \frac{h''}{2}\right) \quad (69)$$

where

$$\nu_1 = \left(\frac{\sinh(\xi_{y,2}h'')}{\sinh(\xi_{y,1}h)}\, e^{\gamma_{xz}}\right)^* \cdot \left(\frac{\sinh(\xi_{y,2}h'')}{\sinh(\xi_{y,1}h)}\left(\frac{\xi_{y,2}^2+K_0^2}{jK_0\gamma_x}\right) e^{\gamma_{xz}}\right) \quad (70)$$

$$\nu_2 = \left(\frac{\xi_{y,2}^2 + K_0^2}{jK_0\gamma_x}\right) e^{\gamma_{xz}}\left(e^{\gamma_{xz}}\right)^* \quad (71)$$

$$\nu_3 = \left(\frac{\cosh(\xi_{y,2}h'')}{\sinh(\xi_{y,1}h)}\left(\frac{\xi_{y,2}^2+K_0^2}{j\omega\epsilon_0\epsilon_r\gamma_x}\right) e^{\gamma_{xz}}\right)^* \cdot \left(\sqrt{\mu_0/\epsilon_0}\,\frac{\cosh(\xi_{y,2}h'')}{\cosh(\xi_{y,1}h)} e^{\gamma_{xz}}\right) \quad (72)$$

$$\nu_4 = \left(\frac{\xi_{y,2}^2 + K_0^2}{j\omega\epsilon_0\gamma_x}\, e^{\gamma_{xz}}\right)^* \sqrt{\mu_0/\epsilon_0}\, e^{\gamma_{xz}} \quad (73)$$

Equations (9)-(73) are detailed in [4]. Equations for the coupled microstrip lines and CBCW are similar to these presented here and are also detailed in [4].

III. NUMERICAL RESULTS

Numerical results presented in this section were obtained by a computer program on a personal computer. In Fig. 3 the dispersive characteristics for a shielded microtrip are presented. Along with de quasi-TEM mode, higher order modes are considered. When compared to results of [5], a good agreement is observed.

In Fig. 4 the dispersive characteristics are presented for open coupled microstrip lines. For the cases considered (ϵ_r=2.35 and ϵ_r=9.7), the results obtained are in accordance with the ones obtained in [6].

In Fig. 5 results are presented for a boxed CBCW. The dispersive characteristics for the quasi-TEM mode are presented for two different strips spacing (S=0.10mm and S=0.40mm). When compared to results of [7], obtained by the usual TRT, a good agreement is observed.

IV. CONCLUSIONS

In this work, a modified formulation of the transverse resonance technique (MTRT) is presented, which is a versatile technique to compute dispersive characteristics of transmission structures. With the MTRT proposed formulation, mode solution identification requires less work, especially when higher order modes are considered. The complete equation set is described. Numerical results are presented for dispersive characteristics of microstrip lines, coupled

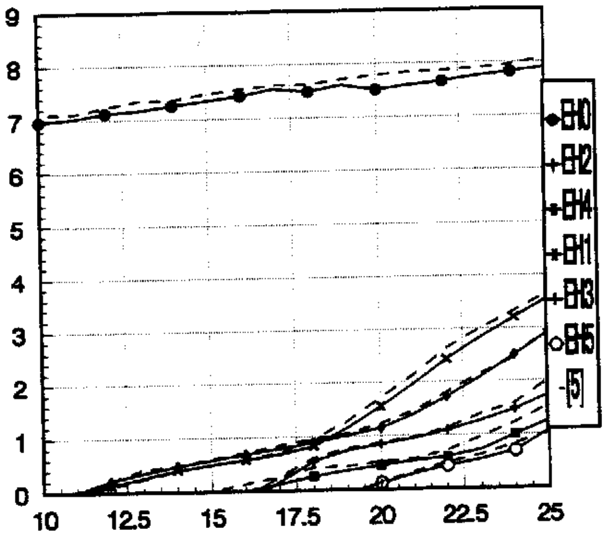

H=L=12.7mm, h=W=1.27mm, ϵ_r=8.875

Figure 3: ϵ_{eff} x frequency (GHz)

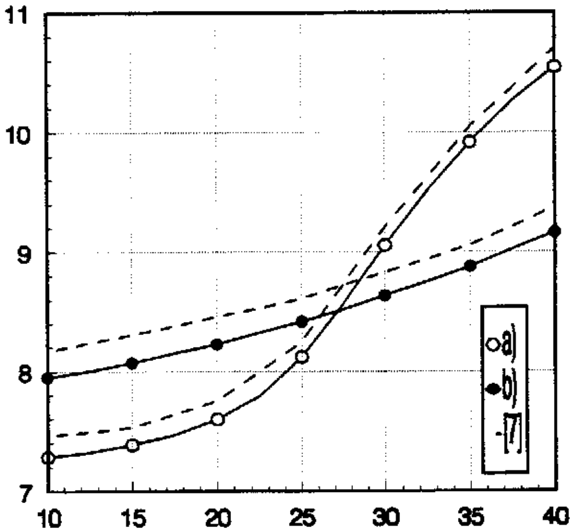

a) H=L=2.5mm, h=0.20mm, S=W=0.10mm, ϵ_r=12.9
b) H=L=2.5mm, h=0.20mm, S=4W=0.40mm, ϵ_r=12.9

Figure 5: ϵ_{eff} x frequency (GHz)

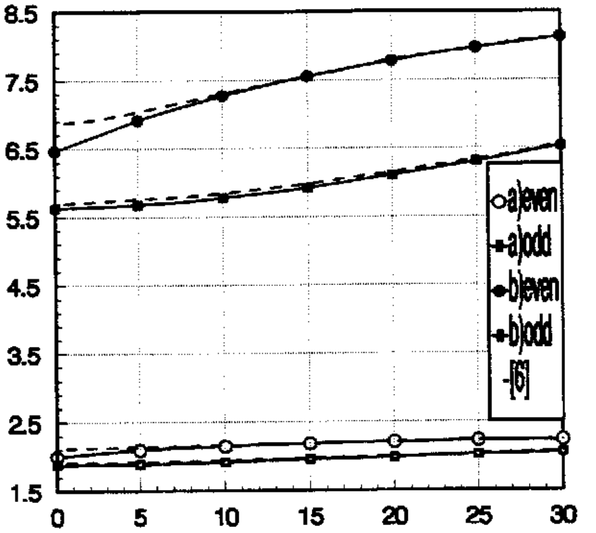

a) h=0.79mm, W=3.16mm, $\frac{S}{2}$=0.395mm, ϵ_r=2.35
b) h=0.64mm, W=0.48mm, $\frac{S}{2}$=0.32mm, ϵ_r=9.7

Figure 4: ϵ_{eff} x frequency (GHz)

microstrip lines and CBCW. When compared to results obtained by other methods, a good agreement is observed.

References

[1] Tatsuo Itoh, editor. *Numerical Techniques for Microwave and Millimeter-Wave Passive Structures.* John Wiley and Sons, Inc., New York, New York, 1989.

[2] R. Sorrentino. *Transverse Resonance Technique - in Numerical Techniques for Microwave and Millimeter-Wave Passive Structures.* chap. 11, T. Itoh, Ed., John Wiley and Sons, Inc., New York, New York, 1989.

[3] H. Baudrand. *Méthodes Numériques en Propagation.* E.N.S.E.E.I.H.T., Toulouse, France, 1992.

[4] Alfrêdo Gomes Neto. *An Alternative Formulation of the Transverse Resonance Technique (in Portuguese).* Dr. Tese, UFPB, Campina Grande, Paraíba, Brazil, December 1994.

[5] Eikichi Yamashita and Kazuhiko Atsuki. "Analysis of microstrip-like transmission lines by nonuniform discretization of integral equations". *IEEE Transactions on Microwave Theory and Techniques*, 24:195–200, April 1976.

[6] M. Kirschning and R. H. Jansen. "Accurate wide-range design equations for the frequency-dependent characteristic of parallel coupled microstrip lines". *IEEE Transactions on Microwave Theory and Techniques*, 32:83–90, January 1984.

[7] H. Baudrand, F. Bouzidi, D. Bajon, and V. Fouad Hanna. "Analysis of conductor-backed coplanar waveguide". In *23rd European Microwave Conference Proceedings*, pages 627–630, Madrid, Spain, September 1993.